AGU PUBLICATIONS

Geophysical Research Letters

RESEARCH LETTER
10.1002/2016GL069416

High atmospheric demand for water can limit forest carbon uptake and transpiration as severely as dry soil

Benjamin N. Sulman[1,2,3], D. Tyler Roman[1,4], Koong Yi[1], Lixin Wang[5], Richard P. Phillips[2], and Kimberly A. Novick[1]

[1]School of Public and Environmental Affairs, Indiana University, Bloomington, Indiana, USA, [2]Department of Biology, Indiana University, Bloomington, Indiana, USA, [3]Program in Atmospheric and Oceanic Sciences, Department of Geosciences, Princeton University, Princeton, New Jersey, USA, [4]U.S. Department of Agriculture, Forest Service, Northern Research Station, Grand Rapids, Minnesota, USA, [5]Department of Earth Sciences, Indiana University-Purdue University at Indianapolis, Indianapolis, Indiana, USA

Key Points:
- Forest transpiration and photosynthesis respond to fluctuations in both vapor pressure deficit and soil moisture
- Elevated VPD can reduce photosynthesis by the same magnitude as soil drying to levels typical of droughts
- Rising VPD due to climatic warming could drive drought-like flux responses in forests even if soil moisture does not decrease

Supporting Information:
- Supporting Information S1
- Data Set S1
- Data Set S2

Correspondence to:
B. N. Sulman,
bsulman@princeton.edu

Citation:
Sulman, B. N., D. T. Roman, K. Yi, L. Wang, R. P. Phillips, and K. A. Novick (2016), High atmospheric demand for water can limit forest carbon uptake and transpiration as severely as dry soil, *Geophys. Res. Lett.*, *43*, 9686–9695, doi:10.1002/2016GL069416.

Received 1 MAY 2016
Accepted 7 SEP 2016
Accepted article online 10 SEP 2016
Published online 29 SEP 2016

Abstract When stressed by low soil water content (SWC) or high vapor pressure deficit (VPD), plants close stomata, reducing transpiration and photosynthesis. However, it has historically been difficult to disentangle the magnitudes of VPD compared to SWC limitations on ecosystem-scale fluxes. We used a 13 year record of eddy covariance measurements from a forest in south central Indiana, USA, to quantify how transpiration and photosynthesis respond to fluctuations in VPD versus SWC. High VPD and low SWC both explained reductions in photosynthesis relative to its long-term mean, as well as reductions in transpiration relative to potential transpiration estimated with the Penman-Monteith equation. Flux responses to typical fluctuations in SWC and VPD had similar magnitudes. Integrated over the year, VPD fluctuations accounted for significant reductions of GPP in both nondrought and drought years. Our results suggest that increasing VPD under climatic warming could reduce forest CO_2 uptake regardless of changes in SWC.

1. Introduction

Forests are the largest terrestrial carbon (C) sink globally and an important source of atmospheric water vapor over land. In forested temperate regions, where annual net carbon uptake and evapotranspiration (ET) are large [*Albani et al.*, 2006; *Sanford and Selnick*, 2013], increases in the intensity and frequency of droughts owing to rising temperatures and reduced precipitation can reduce CO_2 removal from the atmosphere [*Ciais et al.*, 2005; *Brzostek et al.*, 2014], representing a positive climate change feedback [*Zhao and Running*, 2010; *van der Molen et al.*, 2011; *Trenberth et al.*, 2013]. Changes in energy and water vapor fluxes related to land use change can also influence climate at regional scales [*Sahin and Hall*, 1996; *Chase et al.*, 2000; *Pielke et al.*, 2002; *Brown et al.*, 2005; *Juang et al.*, 2007; *Ford et al.*, 2011; *Bagley et al.*, 2012; *Wang et al.*, 2014]. In addition, recent severe drought events have raised concerns of widespread tree mortality under climatic warming [*Allen et al.*, 2010; *Anderegg et al.*, 2012; *Williams et al.*, 2013]. Consequently, forest responses to changing environmental conditions can have profound effects on both regional and global climate [*Bonan*, 2008; *Jasechko et al.*, 2013].

Numerous studies have explored the C consequences of water stress by investigating extended periods of low precipitation [e.g., *Ciais et al.*, 2005; *Schwalm et al.*, 2012] or by reducing precipitation experimentally [e.g., *Hanson et al.*, 2001; *Beier et al.*, 2012; *Gimbel et al.*, 2015]. While these studies have greatly improved our understanding of ecosystem sensitivities to water availability [*Bréda et al.*, 2006; *van der Molen et al.*, 2011; *Vicca et al.*, 2012], their focus on soil water content (SWC) represents a single dimension of how forests experience water stress. In fact, there is ample evidence that plants are sensitive to changes in both soil water *supply* (driven by SWC) and atmospheric *demand* (driven by vapor pressure deficit, VPD). As VPD directly drives water flux across the stomatal interface, plants close their stomata to prevent excessive water loss under high VPD conditions [*Oren et al.*, 1999; *Buckley*, 2005; *Ruehr et al.*, 2014; *Novick et al.*, 2016; *McAdam et al.*, 2016]. While changes in VPD and SWC are often correlated at annual time scales [*Brzostek et al.*, 2014], these correlations mask decoupling of VPD and SWC at finer temporal scales: soils generally dry over periods of several days or weeks, while VPD can change rapidly over hourly time scales. As a result, VPD-driven drought-like water stress can occur even when SWC is not limiting.

Because VPD increases with warming even if relative humidity remains constant, climatic warming is expected to significantly increase VPD in the future [*Williams et al*., 2013]. It is critically important to understand how these increases in VPD will affect plant physiological functioning under climatic change [*Allen et al*., 2010; *Anderegg et al*., 2015; *McDowell and Allen*, 2015]. While ecosystem-scale impacts of severe droughts have been extensively documented [e.g., *Zhao and Running*, 2010; *Brzostek et al*., 2014] and flux responses to changing atmospheric conditions have been well studied at the leaf scale [*Oren et al*., 1999; e.g., *Buckley*, 2005; *Katul et al*., 2009], studies that quantify the relative roles of atmospheric and soil components of drought in determining ecosystem-scale flux responses are largely absent from the literature. This knowledge gap impedes comprehensive mechanistic understanding of forest vulnerability to drought and hinders predictions of forest responses to climatic changes.

We used a 13 year record (2001–2013) of CO_2 and water vapor fluxes from the Morgan Monroe State Forest (MMSF) Ameriflux site, in combination with 3 year records of weekly canopy leaf gas exchange and continuous sap flow measurements, to investigate the responses of photosynthesis and transpiration to atmospheric (VPD) and soil (SWC) components of hydrological stress. Our goals were (1) to separate and compare the effects of VPD and SWC on transpiration and photosynthesis and (2) to quantify the integrated flux impacts of fluctuations in VPD and SWC at annual time scales. Achieving these goals will advance our understanding of forest vulnerabilities to hydrological and climatic changes, inform interpretation of experimentally simulated droughts in forests, and improve modeling of forest carbon and water cycle feedbacks to climatic changes.

2. Methods

2.1. Site Description

Measurements were conducted at the MMSF Ameriflux site (Ameriflux code US-MMS; 39.32°N, 86.41°W). The site is located in a deciduous broadleaf forest with a mean canopy height of approximately 27 m and a stand age of 80–90 years. The dominant tree species in the forest are sugar maple (*Acer saccharum*), tulip poplar (*Liriodendron tulipifera*), sassafras (*Sassafras albidum*), white oak (*Quercus alba*), black oak (*Quercus velutina*), and red oak (*Quercus rubra*). The ecosystem is representative of deciduous forests covering large areas in eastern North America, and the forest species composition is typical of other hardwood forests in the region. The soil type is Typic Dystrochrepts dominated by the Berks-Weikert complex, defined as a well-drained silt loam [*Dragoni et al*., 2010]. For additional details about the site, see *Schmid et al*. [2000].

2.2. Eddy Covariance and Meteorological Measurements

Ecosystem-atmosphere fluxes of heat, water vapor, and CO_2 have been measured using the eddy covariance (EC) method at the site since 1998 at heights of 46 m, 34 m, and 2 m. The 2 m subcanopy flux station is located approximately 20 m from the main tower. Each flux station includes a sonic anemometer (CSAT3, Campbell Scientific Inc., Logan, UT) and a connection to a closed-path infrared gas analyzer (LI-7000, LI-COR Inc., Lincoln, NE) at the base of the tower. Wind and gas concentration measurements are collected at a rate of 10 Hz and processed into fluxes using standard EC techniques at a 1 h time scale (see *Schmid et al*. [2000] for flux processing details). Fluxes from the 46 m flux station were corrected for high-frequency spectral losses resulting from the long tube length (see supporting information (SI) for details). Meteorological measurements included air and soil temperatures, relative humidity, photosynthetically active radiation (PAR), net shortwave and longwave radiation, and precipitation. VPD was calculated using observed air temperature and humidity. Volumetric soil water content (SWC, $m^3\ m^{-3}$) in the first 30 cm of soil depth was monitored using time domain reflectometer (TDR) probes (CS615 and CS616, Campbell Scientific Inc., Logan, UT) and calibrated using gravimetric samples collected weekly at four TDR monitoring locations. Measurements were averaged between the locations to produce an average soil moisture value representative of the flux tower footprint. Soil water potential (Ψ_S), which is more tightly coupled to plant water stress, was calculated from SWC using a relationship developed for the MMSF site by *Wayson et al*. [2006].

Transpiration (T_r) was estimated by subtracting subcanopy (2 m) ET from above-canopy (46 m) ET, assuming that water vapor fluxes from below 2 m were dominated by evaporation and that nonsoil evaporation was negligible. Because evaporation from leaf and stem surfaces can contribute significantly to ET immediately following precipitation, data from within 2 days following precipitation events were excluded from the analysis. This ET partitioning method was recently compared with an alternative method based on flux-variance similarity, and both yielded similar estimates of transpiration at the site [*Sulman et al*., 2016].

Net ecosystem exchange of CO_2 (NEE) was partitioned into gross primary production (GPP) and ecosystem respiration (ER) using a nonlinear regression method that has been applied in previous studies at the MMSF site [*Schmid et al*., 2000; *Dragoni et al*., 2010] and has been shown to agree well with other approaches [*van Gorsel et al*., 2009]. Nighttime NEE was assumed to equal ER and used to parameterize an exponential function of temperature. This modeled ER was then subtracted from daytime NEE in order to estimate GPP. Years 2001–2013 were used for the GPP portion of the analysis. Issues with soil moisture measurements prevented the use of data prior to 2001. The transpiration portion of the analysis was limited to years 2004–2013, when subcanopy ET measurements were available. Sap flow and leaf gas exchange measurements were also collected in 2011–2013 as supporting data (see SI for methodological details of sap flow [*Marshall*, 1958; *Green et al*., 2003; *Caylor and Dragoni*, 2009] and leaf gas exchange [*Roman et al*., 2015]).

2.3. Potential Transpiration and GPP

Potential transpiration was calculated using the Penman-Monteith equation driven by measured net radiation, VPD, air temperature, and wind speed from the EC tower:

$$T_{\mathrm{PM}} = \frac{S(R_{\mathrm{net}} - G) + C_p \rho_a g_a \mathrm{VPD}}{\lambda \rho_w \left(S + \gamma \left(1 + \frac{g_a}{g_{max}} \right) \right)}, \quad (1)$$

where T_{PM} is potential transpiration using the Penman-Monteith equation, S is the slope of the water vapor saturation function, R_{net} is net radiation, G is soil heat flux, C_p is specific heat capacity of dry air, g_a is aerodynamic conductance (proportional to wind speed), λ is latent heat of vaporization of water, ρ_w is density of water, ρ_a is density of air, γ is the psychometric constant, and g_{max} is maximum surface conductance. A single value representing maximum surface conductance was calculated by fitting the equation to observed ET during periods of high light availability (PAR $>$ 1200 μmol m^{-2} s^{-1}), adequate soil moisture (SWC above its 75th percentile), and low VPD (between 0.8 and 1.2 kPa) during the growing season (between Julian day 150 and 250 of each year, when site leaf area index was relatively stationary and evaporation was small relative to transpiration) over the entire 13 year record. Using a single value of g_{max} reduced the influence of interannual variations such as the 2012 drought on estimates of potential flux and allowed T_{PM} to be treated as a representative long-term metric for this ecosystem.

The Penman-Monteith equation explicitly accounts for the fact that in the absence of soil moisture or atmospheric limitations to stomatal functioning, T_r is linearly related to VPD, reflecting the direct relationship between VPD and evaporation rate [*Dalton*, 1802]. When VPD is high, the water vapor concentration gradient between the leaf interior and the atmosphere is steep, and water diffuses out of stomata more quickly. Thus, by using the Penman-Monteith equation to determine T_{PM}, we can isolate the extent to which stomatal closure under high VPD and low soil moisture reduces T_r from its potential rate.

In addition to estimating reductions in T_r relative to its potential rate, we quantified variations in T_r and GPP relative to their long-term mean values. We calculated long-term average T_r (T_{norm}) and GPP ($\mathrm{GPP}_{\mathrm{norm}}$) by averaging the annual time series of EC measurements across all years. This produced a "normal" time series so that each hour of the year could be compared to multiyear average values for that hour.

2.4. Statistical Analysis

In order to quantify the relative contributions of VPD and SWC to variations in GPP and T_r, we applied a linear statistical model that included soil water potential (Ψ_S) and ln(VPD) as predictors and the ratios of GPP and T_r to their multiyear average values ($\mathrm{GPP}/\mathrm{GPP}_{\mathrm{norm}}$ and T_r/T_{norm}, respectively) as response variables. We also applied the model to the ratio of T_r/T_{PM}. The logarithmic transformation of VPD was based on previous studies [*Oren et al*., 1999]. Ψ_S was used rather than SWC in the statistical analysis because it is a more accurate representation of the role of soil water in the soil-plant-atmosphere continuum and gave a more accurate fit to the observations. However, SWC is used in the figures for ease of interpretation. The full statistical model had the form

$$F = C_1 + C_2 \ln(\mathrm{VPD}) + C_3 \Psi_S + C_4 \ln(\mathrm{VPD}) \Psi_S, \quad (2)$$

where F is T_r/T_{norm}, T_r/T_{PM}, or GPP/GPP$_{norm}$, and C_1 through C_4 are the regression coefficients. The regressions were calculated using the robust linear model method of the Statsmodels python package (version 0.6.1) [*Seabold and Perktold*, 2010].

Annual flux anomalies were calculated by summing the difference between each flux and its multiyear average time series over each year:

$$\Delta F = \sum \left[F_{obs} - F_{norm}\right], \tag{3}$$

where ΔF is annual flux anomaly, F_{obs} is observed flux, and F_{norm} is the multiyear average flux time series. Modeled annual anomalies were calculated by integrating the difference between the statistically modeled time series and F_{norm} over each year:

$$\Delta F_{mod} = \sum \left[F_{norm}(C_1 + C_2 \ln(\text{VPD}) + C_3\Psi_S + C_4\ln(\text{VPD})\Psi_S) - F_{norm}\right], \tag{4}$$

where ΔF_{mod} is modeled flux anomaly. Only daytime measurements were included in these calculations. Because the logarithmic VPD dependence of the model made it very sensitive to low values of VPD, time periods when VPD was less than 1 kPa were assumed to have zero contribution to limitation of fluxes. Contributions of individual model terms to annual total fluxes were calculated using the appropriate terms and coefficients from equation (2) and normalized by multiyear average flux:

$$\Delta F_{Intercept} = 100(C_1 - 1.0), \tag{5}$$

$$\Delta F_{VPD} = 100\frac{\sum \left[F_{norm}C_2 \ln(\text{VPD})\right]}{\sum F_{norm}}, \tag{6}$$

$$\Delta F_{\Psi_S} = 100\frac{\sum \left[F_{norm}C_3\Psi_S\right]}{\sum F_{norm}}, \tag{7}$$

$$\Delta F_{\text{VPD}\times\Psi_S} = 100\frac{\sum \left[F_{norm}C_4\Psi_S\ln(\text{VPD})\right]}{\sum F_{norm}}, \tag{8}$$

where $\Delta F_{Intercept}$, ΔF_{VPD}, ΔF_{Ψ_S}, and $\Delta F_{\text{VPD}\times\Psi_S}$ represent percentage differences in flux relative to F_{norm} due to the model intercept, VPD, Ψ_S, and the VPD $\times$ Ψ_S interaction, respectively. Annual anomalies and the contributions of different terms to changes in T_r were also calculated relative to T_{PM}, using equations (3)–(8) with T_{PM} in place of T_{norm}.

3. Results

3.1. Meteorology and Fluxes Over the Study Period

The MMSF site climate is characterized by cold winters and warm, humid summers. Growing-season precipitation is highest from March to June and lowest from July to September. SWC is typically high in winter and spring and declines over the growing season beginning in April and reaching a minimum in September before rising again in autumn (Figure S1). From 1999 to 2014, annual average SWC has declined, and VPD has increased [*Brzostek et al.*, 2014]. The site experienced droughts in 2002, 2007, 2010, and 2011 and an especially severe drought in 2012 [*Roman et al.*, 2015]. Soil water content was anomalously low during all drought years, but VPD was exceptionally high during the 2012 drought (Figure S1). T_r and GPP declined significantly during the 2012 drought before recovering as conditions eased later in the growing season. Average GPP over the study period was approximately 1.4 kg C m^{-2} yr^{-1}, and average annual T_r was approximately 490 mm yr^{-1}. Evaporation estimated using subcanopy fluxes was generally less than 5% compared to T_r during the growing season.

VPD and SWC were negatively correlated ($r = -0.47$ for daily values), so most high-VPD days occurred when soil was also dry. However, high VPD occurred even during periods when soil was relatively wet (Figure S2b), exceeding 2 kPa on approximately 9% of days with SWC > 0.3 m^3 m^{-3}.

3.2. SWC and VPD Relationships With Fluxes

T_r/T_{PM} declined with increasing VPD at all soil moisture levels (Figure 1b) and increased at the same rate with Ψ_S at all VPD levels (Figure 1e). Increases in VPD were correlated with increasing T_r/T_{norm}, but the rate of

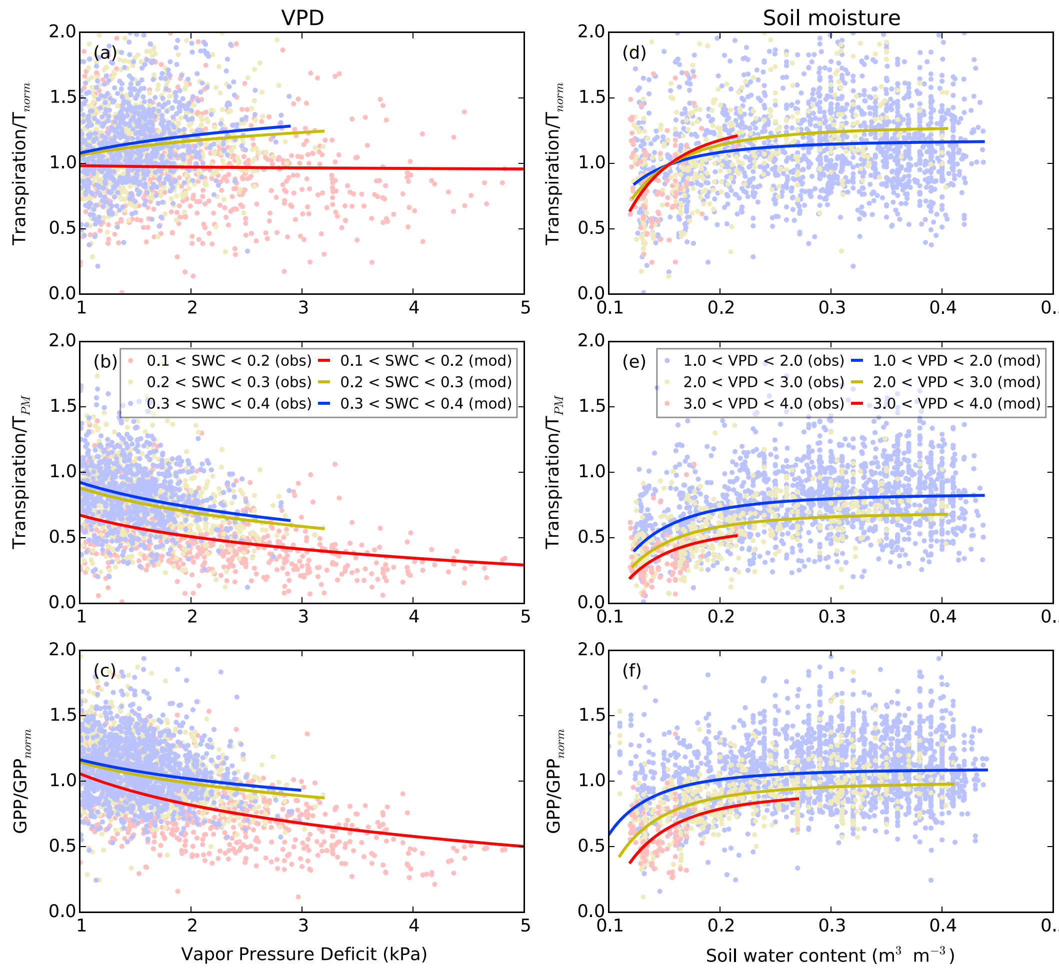

Figure 1. Measured and modeled fluxes as a function of VPD and SWC. (a–c) Relationships with VPD and (d–f) relationships with SWC. Rows show different normalized fluxes: T_r/T_{norm} (Figures 1a and 1d); T_r/T_{PM} (Figures 1b and 1e); and GPP/GPP$_{\mathrm{norm}}$ (Figures 1c and 1f). Lines show the statistical regression, and symbols show measured values. Colors are matched between lines and symbols to show the SWC levels (Figures 1a–1c) and VPD levels (Figures 1d–1f).

increase was highly dependent on SWC (Figure 1a). Under the driest soil conditions (SWC $< 0.2\,\mathrm{m^3\,m^{-3}}$), T_r/T_{norm} was insensitive to VPD. Similarly, T_r/T_{norm} was most sensitive to SWC under high VPD conditions (Figure 1d). The responses of GPP/GPP$_{\mathrm{norm}}$ to VPD and Ψ_S were very similar to those of T_r/T_{PM}, decreasing with increasing VPD at all soil moisture levels. Similar relationships with VPD were observed in both sap flow (Figure S3) and leaf gas exchange (Figure S4) measurements. However, while the Ψ_S relationships observed in EC data were consistent with sap flow data, leaf gas exchange transpiration was insensitive to Ψ_S. Pronounced SWC effects on EC fluxes were limited to periods when SWC was below approximately $0.2\,\mathrm{m^3\,m^{-3}}$. Interactions between ln(VPD) and Ψ_S were statistically significant for EC-based GPP/GPP$_{\mathrm{norm}}$ and T_r/T_{norm}, but not for T_r/T_{PM}. The interaction was positive in both cases, meaning that the decline in GPP with increasing VPD was weaker under wetter soil conditions (Figure 1c), while T_r/T_{norm} increased more rapidly with VPD under wetter soil conditions (Figure 1a).

When integrated over the year, the observed statistical relationships of GPP/GPP$_{\mathrm{norm}}$ with VPD and Ψ_S explained most of the interannual variability in GPP ($r^2 = 0.53$) and T_r relative to T_{PM} ($r^2 = 0.86$), although they overestimated flux magnitudes relative to observations. Correlation was lower for T_r relative to T_{norm} ($r^2 = 0.20$) (Figure 2). Based on the statistical model, VPD had a larger impact than SWC on GPP and T_r except in 2011 and 2012 (Figures 2e and 2f). Modeled contributions of VPD and SWC were very similar between these flux metrics. In contrast, the model based on T_r/T_{norm} suggested that VPD alone would increase fluxes in all years. However, statistical interactions between VPD and Ψ_S counteracted the VPD effect in drought

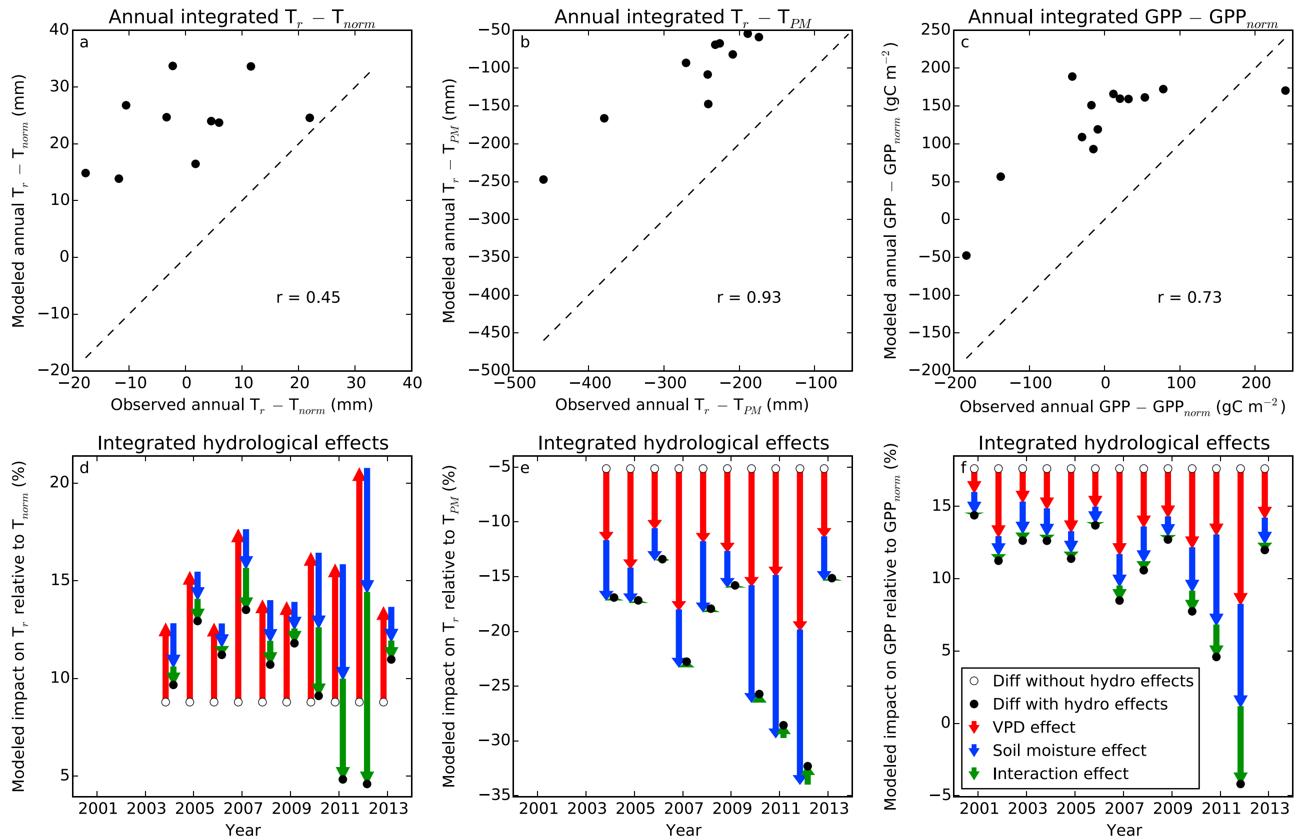

Figure 2. Interannual variations in fluxes and fractions attributed to different hydrological drivers by the statistical model. (a–c) Modeled (ΔF_{mod}; equation (4)) and observed (ΔF; equation (3)) annual integrated difference between T_r and T_{norm} (Figure 2a), T_r and T_{PM} (Figure 2b), and GPP and GPP_{norm} (Figure 2c). Dashed lines show 1-1 relationships. (d–f) Annual integrated contribution of each statistical model term to variations in T_r relative to T_{norm} (Figure 2d), T_r relative to T_{PM} (Figure 2e), and GPP relative to GPP_{norm} (Figure 2f). Red, blue, and green arrows show effects of VPD, soil moisture, and their interaction, respectively (equations (6)–(8)). White circles show $\Delta F_{Intercept}$ (equation (5)). Black circles show the combined effect of all statistical model terms (equivalent to ΔF_{mod}). When this total is greater than zero, the integrated modeled flux is greater than the integrated multiyear mean flux.

years, leading to substantial reductions in transpiration (Figure 2d). Integrated modeled fluxes including hydrological effects were generally greater than integrated multiyear mean fluxes, reflecting the overestimates of integrated flux magnitudes. Based on the statistical model, VPD explained 55% of hydrologically driven reduction of GPP over the study period, compared to 33% for SWC and 13% for their interaction. Excluding the drought years of 2011 and 2012, VPD explained 61% of GPP reduction, while SWC was responsible for 31%.

4. Discussion

Ecosystem-scale transpiration and photosynthesis were significantly correlated with both VPD and soil moisture (Figure 1). A statistical model based on these relationships suggested that VPD was a primary contributor to interannual variability in photosynthesis and transpiration at our temperate forest site over a 13 year period (Figure 2). These results highlight the importance of VPD in determining plant-controlled ecosystem fluxes and their responses to climatic changes.

Relative to multiyear-average values, T_r increased with increasing VPD under nonlimiting SWC conditions and stayed constant when soils were dry (Figure 1a). Because increasing VPD increases the water vapor concentration gradient from the leaf to the atmosphere, it is expected to accelerate transpiration. However, observed T_r responses were less than the increases that would be expected from this diffusion effect alone (Figure 1b), suggesting stomatal limitations to transpiration. The effects of declining stomatal conductance on T_r were particularly apparent when actual T_r was compared to potential transpiration calculated with the Penman-Monteith equation, which accounts for VPD effects on the water vapor concentration gradient (equation (1)). T_r/T_{PM} declined with increasing VPD at approximately the same rate regardless of soil moisture. Because photosynthesis and transpiration are both mediated by stomatal conductance, T_r/T_{PM} and GPP/GPP_{norm} should have similar responses to environmental drivers that affect stomatal conductance, though those responses may be affected by variations in water use efficiency. In fact, T_r/T_{PM} and GPP/GPP_{norm} had very similar responses to changes in both VPD and SWC, which supports a robust finding that reductions in stomatal conductance driven by increasing VPD had significant effects on GPP, even under nonlimiting soil moisture conditions. These conclusions are further supported by the similar responses of T_r/T_{PM} and GPP/GPP_{norm} to VPD in leaf gas exchange measurements.

Declines of T_r/T_{PM} and GPP/GPP_{norm} with SWC became significant only at SWC values below approximately 0.2 $m^3\ m^{-3}$, representing less than 15% of growing season days in the record. This was due to the nonlinear relationship between SWC and plant water limitation, as encapsulated by Ψ_S (Figures 1e and 1f). At higher values of SWC, water potential is not limiting, and a small decline in SWC will not drive a significant plant physiological response. In contrast, increases in VPD significantly reduced GPP/GPP_{norm} and T_r/T_{PM} at VPD levels as low as 1.5 kPa (Figures 1b and 1c). VPD exceeded 1.5 kPa during almost 55% of all growing season days and during approximately 30% of growing season days excluding periods when SWC was below 0.25 $m^3\ m^{-3}$ (Figure S2c). An increase in VPD from 1.5 to 2.5 kPa reduced GPP and T_r by approximately as much as a change in SWC from a wet state of 0.35 $m^3\ m^{-3}$ to a typical drought level of 0.15 $m^3\ m^{-3}$. Integrated over the year, these relationships suggest that high VPD levels significantly reduced total GPP relative to its potential maximum values even in nondrought years (Figure 2f). During the severe 2012 drought, VPD contributed as much as SWC to the unusually strong suppression of GPP and T_r (Figures 2d–2f). This is consistent with recent studies indicating that high VPD aggravates drought effects in forests [*Adams et al*., 2009; *Katul et al*., 2009; *Williams et al*., 2013; *Ruehr et al*., 2014; *McDowell and Allen*, 2015]. Because VPD can change significantly over short time scales and can temporarily reach high levels without associated soil drying, short-term drought-like ecosystem responses could occur during periods that are not identified as droughts by indices like the Palmer Drought Severity Index (PDSI), which integrate over longer time scales and respond slowly to meteorological changes [*Trenberth et al*., 2013]. *Sheffield et al*. [2012] found that PDSI-based studies overestimated the occurrence of droughts in the twentieth century because they relied on temperature to predict evaporation rather than including VPD. While temperature is correlated with humidity and other drivers of drought stress at longer time scales of weeks or months, these slowly varying indices do not capture the fast time scale variations in VPD that can also limit photosynthesis according to our results.

Our use of multiyear averages as well as the Penman-Monteith equation could have introduced error into this analysis. The Penman-Monteith equation is a physically comprehensive model of potential evapotranspiration, including a full set of accepted mechanistic drivers of evapotranspiration including temperature, VPD, radiation, and wind speed. Previous studies have argued that the Penman-Monteith model yields more physically accurate predictions of potential evapotranspiration than models that only include temperature and radiation [*Sheffield et al*., 2012]. However, the temperature- and radiation-based Priestley-Taylor model has been shown to yield accurate predictions of actual evapotranspiration [e.g., *Lu et al*., 2005; *Sumner and Jacobs*, 2005]. A version of our analysis conducted using the Priestley-Taylor model yielded similar results to the analysis based on multiyear-average transpiration. We focused on multiyear average fluxes rather than the Priestley-Taylor model in order to use observed fluxes when possible. However, the 13 years of GPP and 10 years of transpiration may not have been enough to overcome the high hourly variability inherent to EC measurements. Based on variability between years, the standard deviation of the mean for multiyear average fluxes at the hourly scale was approximately 10–15%. The model overestimated total fluxes relative to multiyear averages (Figure 2). This was likely due to a high intercept value that resulted from focusing on conditions when fluxes were not severely limited by factors such as light and temperature. However, the interannual patterns of hydrological effects are supported by the strong relationships shown in Figure 1.

Our results primarily focused on bulk fluxes of water vapor and CO_2 between the forest canopy and the atmosphere. Water flow from soils, through trees, to the atmosphere is also controlled by aspects of tree physiology such as stem water storage and xylem water potential. Supporting measurements of T_r/T_{PM} using leaf gas exchange and sap flow measurements (Figures S3 and S4) had very similar responses to VPD compared to EC measurements, demonstrating the consistent scaling of this response from leaf, to tree, to ecosystem scale. Leaf-level photosynthesis responses were also very similar to those observed in EC measurements. However, leaf fluxes were insensitive to SWC, while sap flow and EC fluxes were jointly controlled by SWC and VPD. These differing responses are consistent with hydrological flows across the soil-tree-atmosphere continuum. Sap flow has been observed to lag transpiration due to changes in stem water storage [*Hogg et al*., 1997], and nocturnal water uptake can represent a significant fraction of total water uptake, as storage reserves depleted during the day are refilled [*Oishi et al*., 2008]. Water supply to leaves can be temporarily supported by depletion of stem water storage, decoupling leaf water from SWC. The leaf responses were consistent with the results of *Roman et al*. [2015], who observed that the sensitivity of stomatal conductance to VPD of canopy-dominant sugar maple at the site was not affected by soil moisture.

While including some severe droughts, our study focused on continuous responses of fluxes to hydrological drivers and did not investigate strongly nonlinear drought responses such as tree mortality. In contrast to the temporary variations we observed, widespread mortality has long-lasting impacts on forest productivity and structure. While tree mortality during droughts is not yet fully understood and is still the subject of active research [*Klein*, 2015], recent studies suggest that both SWC and VPD contribute to drought mortality [*Anderegg et al*., 2012; *Breshears et al*., 2013]. Vulnerability of trees to drought varies by species [*Choat et al*., 2012] and is influenced by a range of hydraulic traits [*Anderegg et al*., 2016].

Our results represent a case study of a single deciduous forest, and other forests could have different responses resulting from species- or community-level differences in plant physiology. Plants can be divided into isohydric and anisohydric categories based on patterns of stomatal control of leaf water potential [*Tardieu and Simonneau*, 1998]. Isohydric plants maintain leaf water potential by aggressively closing stomata, while anisohydric plants allow it to vary over a wider range. Both isohydric and anisohydric trees are represented at MMSF and have different observed responses to hydraulic stress [*Roman et al*., 2015]. Different relative abundance of isohydric and anisohydric plants in other ecosystems could influence the responses of stand-scale fluxes to VPD and SWC, with anisohydric-dominated ecosystems potentially having weaker responses to changes in VPD. Changes in forest structure and composition or physiological adaptations could also cause changes in forest sensitivity to SWC and VPD over long time scales [*Nicotra et al*., 2010].

These results highlight the importance of including VPD in experiments, models, and analyses related to drought impacts. The importance of drought effects on forest growth and carbon uptake has been well documented [*Ciais et al*., 2005; *van der Molen et al*., 2011; *Schwalm et al*., 2012]. Droughts integrate atmospheric and soil drying but are often identified in terms of soil water availability [e.g., *Hanson and Weltzin*, 2000; *Schwalm et al*., 2012]. Because VPD and soil moisture are often correlated at longer time scales, this approach has historically been successful in diagnosing droughts and their ecosystem effects. While projected impacts of climatic warming on precipitation are uncertain [*Burke and Brown*, 2009; *Kirtman et al*., 2013], there is high confidence that global temperatures and VPD will rise in the future [*Williams et al*., 2013]. Therefore, the importance of VPD in driving hydrological stress, especially during droughts and heat waves, is likely to increase. Our results suggest that in the absence of significant physiological adaptations, increasing occurrence of high VPD episodes could significantly reduce photosynthesis even during nondrought years. Resulting reductions in CO_2 uptake could function as a positive feedback to climatic change. Our results suggest that precipitation manipulation experiments [*Beier et al*., 2012] may underestimate the severity of vegetation drought responses by excluding changes in VPD. While manipulating atmospheric humidity at the ecosystem scale is often infeasible, the role of VPD should be considered when interpreting the results of these experiments. In managed systems, drought mitigation strategies also generally focus on increasing soil moisture through thinning and irrigation [*Linder*, 2000; *Elkin et al*., 2015], which could be less effective under VPD-driven water stress.

5. Conclusions

Long-term eddy covariance measurements showed that variations in GPP and transpiration were correlated with both VPD and SWC. While fluxes responded continuously to increases in VPD, SWC drove substantial flux responses only during severe drought periods. A statistical model based on these relationships suggested that VPD was a primary driver of interannual variations in GPP and transpiration. These results highlight the importance of VPD both as a component of drought and as a driver of carbon and water fluxes under well-watered conditions. In the context of changing climate, our results suggest that warming temperatures could increase future drought impacts on forests. Furthermore, episodes of elevated VPD could reduce CO_2 uptake as temperatures rise, regardless of changes in soil moisture.

Acknowledgments

Special thanks to E. R. Brzostek, S. Scott, A.F. Rahman, D. Dragoni, H. P. Schmid, and S. Grimmond for contributions to the long-term data record at the site. This work benefitted from funding by the Ameriflux Management Project (managed by Lawrence Berkeley National Laboratory with support from the U.S. Department of Energy) and the Indiana University Collaborative Research Grant Program. Additional computing support was provided by the Indiana University Geography Department, and material support was provided by the Indiana University Research and Teaching Preserve. B. Sulman was supported by NOAA/GFDL-Princeton University Cooperative Institute for Climate Science. Thanks to the two anonymous reviewers for their helpful comments. EC and meteorological data are archived in the Ameriflux database (http://ameriflux.ornl.gov/, site code "US-MMS"). Sap flow and leaf gas exchange data are included in SI.

References

Adams, H. D., M. Guardiola-Claramonte, G. A. Barron-Gafford, J. C. Villegas, D. D. Breshears, C. B. Zou, P. A. Troch, and T. E. Huxman (2009), Temperature sensitivity of drought-induced tree mortality portends increased regional die-off under global-change-type drought, *Proc. Natl. Acad. Sci. U.S.A.*, *106*(17), 7063–7066, doi:10.1073/pnas.0901438106.

Albani, M., D. Medvigy, G. C. Hurtt, and P. R. Moorcroft (2006), The contributions of land-use change, CO_2 fertilization, and climate variability to the eastern US carbon sink, *Global Change Biol.*, *12*(12), 2370–2390, doi:10.1111/j.1365-2486.2006.01254.x.

Allen, C. D., et al. (2010), A global overview of drought and heat-induced tree mortality reveals emerging climate change risks for forests, *For. Ecol. Manage.*, *259*(4), 660–684, doi:10.1016/j.foreco.2009.09.001.

Anderegg, W. R. L., J. A. Berry, D. D. Smith, J. S. Sperry, L. D. L. Anderegg, and C. B. Field (2012), The roles of hydraulic and carbon stress in a widespread climate-induced forest die-off, *Proc. Natl. Acad. Sci. U.S.A.*, *109*(1), 233–237, doi:10.1073/pnas.1107891109.

Anderegg, W. R. L., A. Flint, C.-Y. Huang, L. Flint, J. A. Berry, F. W. Davis, J. S. Sperry, and C. B. Field (2015), Tree mortality predicted from drought-induced vascular damage, *Nat. Geosci.*, *8*, 367–371, doi:10.1038/ngeo2400.

Anderegg, W. R. L., T. Klein, M. Bartlett, L. Sack, A. F. A. Pellegrini, B. Choat, and S. Jansen (2016), Meta-analysis reveals that hydraulic traits explain cross-species patterns of drought-induced tree mortality across the globe, *Proc. Natl. Acad. Sci. U.S.A.*, *113*(18), 5024–5029, doi:10.1073/pnas.1525678113.

Bagley, J. E., A. R. Desai, P. A. Dirmeyer, and J. A. Foley (2012), Effects of land cover change on moisture availability and potential crop yield in the world's breadbaskets, *Environ. Res. Lett.*, *7*(1), 014009, doi:10.1088/1748-9326/7/1/014009.

Beier, C., et al. (2012), Precipitation manipulation experiments—Challenges and recommendations for the future, *Ecol. Lett.*, *15*(8), 899–911, doi:10.1111/j.1461-0248.2012.01793.x.

Bonan, G. (2008), Forests and climate change: Forcings, feedbacks, and the climate benefits of forests, *Science*, *320*, 1444–1449.

Bréda, N., R. Huc, A. Granier, and E. Dreyer (2006), Temperate forest trees and stands under severe drought: A review of ecophysiological responses, adaptation processes and long-term consequences, *Ann. For. Sci.*, *63*(6), 625–644, doi:10.1051/forest:2006042.

Breshears, D. D., H. D. Adams, D. Eamus, N. McDowell, D. J. Law, R. E. Will, A. P. Williams, and C. B. Zou (2013), The critical amplifying role of increasing atmospheric moisture demand on tree mortality and associated regional die-off, *Front. Plant Sci.*, *4*, 266, doi:10.3389/fpls.2013.00266.

Brown, A. E., L. Zhang, T. A. McMahon, A. W. Western, and R. A. Vertessy (2005), A review of paired catchment studies for determining changes in water yield resulting from alterations in vegetation, *J. Hydrol.*, *310*, 28–61, doi:10.1016/j.jhydrol.2004.12.010.

Brzostek, E. R., D. Dragoni, H. P. Schmid, A. F. Rahman, D. Sims, C. A. Wayson, D. J. Johnson, and R. P. Phillips (2014), Chronic water stress reduces tree growth and the carbon sink of deciduous hardwood forests, *Global Change Biol.*, *20*(8), 2531–2539, doi:10.1111/gcb.12528.

Buckley, T. N. (2005), The control of stomata by water balance, *New Phytol.*, *168*(2), 275–292, doi:10.1111/j.1469-8137.2005.01543.x.

Burke, E. J., and S. J. Brown (2009), Evaluating uncertainties in the projection of future drought, *J. Hydrometeorol.*, *9*(2), 292–299, doi:10.1175/2007JHM929.1.

Caylor, K. K., and D. Dragoni (2009), Decoupling structural and environmental determinants of sap velocity: Part I. Methodological development, *Agr. Forest Meteorol.*, *149*(3–4), 559–569, doi:10.1016/j.agrformet.2008.10.006.

Chase, T., R. Pielke Sr., T. Kittel, and R. Nemani, and S. W. Running (2000), Simulated impacts of historical land cover changes on global climate in northern winter, *Clim. Dyn.*, *16*, 93–105.

Choat, B., et al. (2012), Global convergence in the vulnerability of forests to drought, *Nature*, *491*, 752–755, doi:10.1038/nature11688.

Ciais, P., et al. (2005), Europe-wide reduction in primary productivity caused by the heat and drought in 2003, *Nature*, *437*(7058), 529–533, doi:10.1038/nature03972.

Dalton, J. (1802), On evaporation. Essay III in: Experimental essays on the constitution of mixed gases; On the force of steam or vapour from water or other liquids in different temperatures; both in a Torrecellian vacuum and in air; on evaporation; and on the expansion of gases by heat, *Mem. Proc. Lit. Phil. Soc. Manchester*, *5*(2), 574–594.

Dragoni, D., H. P. Schmid, C. A. Wayson, H. Potter, C. S. B. Grimmond, and J. C. Randolph (2010), Evidence of increased net ecosystem productivity associated with a longer vegetated season in a deciduous forest in south-central Indiana, USA, *Global Change Biol.*, *17*(2), 886–897, doi:10.1111/j.1365-2486.2010.02281.x.

Elkin, C., A. Giuggiola, A. Rigling, and H. Bugmann (2015), Short-and long-term efficacy of forest thinning to mitigate drought impacts in mountain forests in the European Alps, *Ecol. Appl.*, *25*(4), 1083–1098, doi:10.1890/14-0690.1.

Ford, C. R., S. H. Laseter, W. T. Swank, and J. M. Vose (2011), Can forest management be used to sustain water based-ecosystem services in the face of climate change?, *Ecol. Appl.*, *21*(6), 2049–2067, doi:10.1890/10-2246.1.

Gimbel, K. F., et al. (2015), Drought in forest understory ecosystems—A novel rainfall reduction experiment, *Biogeosciences*, *12*(4), 961–975, doi:10.5194/bg-12-961-2015.

Green, S., B. Clothier, and B. Jardine (2003), Theory and practical application of heat pulse to measure sap flow, *Agron. J.*, *95*(6), 1371–1379, doi:10.2134/agronj2003.1371.

Hanson, P. J., and J. F. Weltzin (2000), Drought disturbance from climate change: response of United States forests, *Sci. Total Environ.*, *262*(3), 205–220, doi:10.1016/S0048-9697(00)00523-4.

Hanson, P. J., J. Donald, E. Todd, and J. S. Amthor (2001), A six-year study of sapling and large-tree growth and mortality responses to natural and induced variability in precipitation and throughfall, *Tree Physiol.*, *21*(6), 345–358, doi:10.1093/treephys/21.6.345.

Hogg, E. H., et al. (1997), A comparison of sap flow and eddy fluxes of water vapor from a boreal deciduous forest, *J. Geophys. Res.*, *102*, 28,929–28,937, doi:10.1029/96JD03881.

Jasechko, S., Z. D. Sharp, J. J. Gibson, S. J. Birks, Y. Yi, and P. J. Fawcett (2013), Terrestrial water fluxes dominated by transpiration, *Nature*, *496*(7445), 347–350, doi:10.1038/nature11983.

Juang, J.-Y., G. G. Katul, M. B. S. Siqueira, P. C. Stoy, and K. Novick (2007), Separating the effects of albedo from eco-physiological changes on surface temperature along a successional chronosequence in the southeastern United States, *Geophys. Res. Lett.*, *34*, L21408, doi:10.1029/2007GL031296.

Katul, G. G., S. Palmroth, and R. Oren (2009), Leaf stomatal responses to vapour pressure deficit under current and CO_2-enriched atmosphere explained by the economics of gas exchange, *Plant Cell Environ.*, *32*(8), 968–979, doi:10.1111/j.1365-3040.2009.01977.x.

Kirtman, B., et al. (2013), Near-term climate change: Projections and predictability, in *Climate Change 2013: The Physical Science Basis. Contribution of Working Group I to the Fifth Assessment Report of the Intergovernmental Panel on Climate Change*, edited by T. F. Stocker et al., Cambridge Univ. Press, Cambridge and New York.

Klein, T. (2015), Drought-induced tree mortality: from discrete observations to comprehensive research, *Tree Physiol.*, *35*(3), 225–228, doi:10.1093/treephys/tpv029.

Linder, M. (2000), Developing adaptive forest management strategies to cope with climate change, *Tree Physiol.*, *20*, 299–307, doi:10.1093/treephys/20.5-6.299.

Lu, J., G. Sun, S. G. McNulty, and D. M. Amatya (2005), A comparison of six potential evapotranspiration methods for regional use in the southeastern United States, *J. Am. Water Resour. Assoc.*, *41*(3), 621–633, doi:10.1111/j.1752-1688.2005.tb03759.x.

Marshall, D. C. (1958), Measurement of sap flow in conifers by heat transport, *Plant Physiol.*, *33*(6), 385–396.

McAdam, S. A. M., F. C. Sussmilch, and T. J. Brodribb (2016), Stomatal responses to vapour pressure deficit are regulated by high speed gene expression in angiosperms, *Plant Cell Environ.*, *39*(3), 485–491, doi:10.1111/pce.12633.

McDowell, N. G., and C. D. Allen (2015), Darcy's law predicts widespread forest mortality under climate warming, *Nat. Clim. Change*, *5*(7), 669–672, doi:10.1038/nclimate2641.

Nicotra, A. B., et al. (2010), Plant phenotypic plasticity in a changing climate, *Trends Plant Sci.*, *15*(12), 684–692, doi:10.1016/j.tplants.2010.09.008.

Novick, K. A., C. F. Miniat, and J. M. Vose (2016), Drought limitations to leaf-level gas exchange: Results from a model linking stomatal optimization and cohesion tension theory, *Plant Cell Environ.*, *39*, 583–596, doi:10.1111/pce.12657.

Oishi, A. C., R. Oren, and P. C. Stoy (2008), Estimating components of forest evapotranspiration: A footprint approach for scaling sap flux measurements, *Agr. Forest Meteorol.*, *148*(11), 1719–1732, doi:10.1016/j.agrformet.2008.06.013.

Oren, R., J. S. Sperry, G. G. Katul, D. E. Pataki, B. E. Ewers, N. Phillips, and K. V. R. Schäfer (1999), Survey and synthesis of intra- and interspecific variation in stomatal sensitivity to vapour pressure deficit, *Plant Cell Environ.*, *22*(12), 1515–1526, doi:10.1046/j.1365-3040.1999.00513.x.

Pielke, R. A., G. Marland, R. A. Betts, T. N. Chase, J. L. Eastman, J. O. Niles, D. D. S. Niyogi, and S. W. Running (2002), The influence of land-use change and landscape dynamics on the climate system: Relevance to climate-change policy beyond the radiative effect of greenhouse gases, *Phil. Trans. R. Soc. A: Math. Phys. Eng. Sci.*, *360*(1797), 1705–1719, doi:10.1098/rsta.2002.1027.

Roman, D. T., K. A. Novick, E. R. Brzostek, D. Dragoni, F. Rahman, and R. P. Phillips (2015), The role of isohydric and anisohydric species in determining ecosystem-scale response to severe drought, *Oecologia*, *179*(3), 641–654, doi:10.1007/s00442-015-3380-9.

Ruehr, N. K., B. E. Law, D. Quandt, and M. Williams (2014), Effects of heat and drought on carbon and water dynamics in a regenerating semi-arid pine forest: A combined experimental and modeling approach, *Biogeosciences*, *11*(15), 4139–4156, doi:10.5194/bg-11-4139-2014.

Sahin, V., and M. J. Hall (1996), The effects of afforestation and deforestation on water yields, *J. Hydrol.*, *178*(1–4), 293–309, doi:10.1016/0022-1694(95)02825-0.

Sanford, W. E., and D. L. Selnick (2013), Estimation of evapotranspiration across the conterminous United States using a regression with climate and land-cover data, *J. Am. Water Resour. Assoc.*, *49*(1), 217–230, doi:10.1111/jawr.12010.

Schmid, H. P., C. S. B. Grimmond, F. Cropley, B. Offerle, and H.-B. Su (2000), Measurements of CO_2 and energy fluxes over a mixed hardwood forest in the mid-western United States, *Agr. Forest Meteorol.*, *103*(4), 357–374, doi:10.1016/S0168-1923(00)00140-4.

Schwalm, C. R., C. A. Williams, K. Schaefer, D. Baldocchi, T. A. Black, A. H. Goldstein, B. E. Law, W. C. Oechel, K. T. Paw U, and R. L. Scott (2012), Reduction in carbon uptake during turn of the century drought in western North America, *Nat. Geosci.*, *5*(8), 551–556, doi:10.1038/ngeo1529.

Seabold, S., and J. Perktold (2010), Statsmodels: Econometric and statistical modeling with Python, *Proc. of the 9th Python in science conf.* http://statsmodels.sourceforge.net

Sheffield, J., E. F. Wood, and M. L. Roderick (2012), Little change in global drought over the past 60 years, *Nature*, *491*(7424), 435–438, doi:10.1038/nature11575.

Sulman, B. N., D. T. Roman, T. M. Scanlon, L. Wang, and K. A. Novick (2016), Comparing methods for partitioning a decade of carbon dioxide and water vapor fluxes in a temperate forest, *Agr. Forest Meteorol.*, *226*, 229–245, doi:10.1016/j.agrformet.2016.06.002.

Sumner, D. M., and J. M. Jacobs (2005), Utility of Penman–Monteith, Priestley–Taylor, reference evapotranspiration, and pan evaporation methods to estimate pasture evapotranspiration, *J. Hydrol.*, *308*(1–4), 81–104, doi:10.1016/j.jhydrol.2004.10.023.

Tardieu, F., and T. Simonneau (1998), Variability among species of stomatal control under fluctuating soil water status and evaporative demand: Modelling isohydric and anisohydric behaviours, *J. Exp. Bot.*, *49*, 419–432.

Trenberth, K. E., A. Dai, G. van der Schrier, P. D. Jones, J. Barichivich, K. R. Briffa, and J. Sheffield (2013), Global warming and changes in drought, *Nat. Clim. Change*, *4*(1), 17–22, doi:10.1038/nclimate2067.

van der Molen, M. K., et al. (2011), Drought and ecosystem carbon cycling, *Agr. Forest Meteorol.*, *151*, 765–773, doi:10.1016/j.agrformet.2011.01.018.

van Gorsel, E., et al. (2009), Estimating nocturnal ecosystem respiration from the vertical turbulent flux and change in storage of CO_2, *Agr. Forest Meteorol.*, *149*, 1919–1930.

Vicca, S., et al. (2012), Urgent need for a common metric to make precipitation manipulation experiments comparable, *New Phytol.*, *195*(3), 518–522, doi:10.1111/j.1469-8137.2012.04224.x.

Wang, L., S. P. Good, and K. K. Caylor (2014), Global synthesis of vegetation control on evapotranspiration partitioning, *Geophys. Res. Lett.*, *41*, 6753–6757, doi:10.1002/2014GL061439.

Wayson, C. A., J. C. Randolph, P. J. Hanson, C. S. B. Grimmond, and H. P. Schmid (2006), Comparison of soil respiration methods in a mid-latitude deciduous forest, *Biogeochemistry*, *80*(2), 173–189, doi:10.1007/s10533-006-9016-8.

Williams, A. P., et al. (2013), Temperature as a potent driver of regional forest drought stress and tree mortality, *Nat. Clim. Change*, *3*, 292–297, doi:10.1038/nclimate1693.

Zhao, M., and S. W. Running (2010), Drought-induced reduction in global terrestrial net primary production from 2000 through 2009, *Science*, *329*(5994), 940–943, doi:10.1126/science.1192666.